

Cleaved Caspase-3 Transcriptionally Regulates Angiogenesis-Promoting Chemotherapy Resistance



Antoine Bernard¹, Sandy Chevrier², Françoise Beltjens², Magalie Dosset¹, Etienne Viltard¹, Anaïs Lagrange¹, Valentin Derangère^{1,3}, Alexandra Oudot⁴, François Ghiringhelli^{1,3}, Bertrand Collin⁴, Lionel Apetoh¹, Olivier Feron⁵, Suzie Chen^{6,7}, Laurent Arnould², Frédérique Végran^{1,3}, and Romain Boidot^{1,2}

Abstract

Caspases are well known for their role in apoptosis. Recently, nonapoptotic roles of caspases have been identified, however, these noncanonical roles are not well documented and the mechanisms involved are not fully understood. Here, we studied the role of cleaved caspase-3 using human- and mouse-proficient caspase-3 cancer cell lines and human-deficient caspase-3 cancer cells. Cleaved caspase-3 functioned as a transcription factor and directly bound to DNA. A DNA-binding domain was identified in the small subunit of caspase-3 and an active conformation was essential for caspase-3 transcriptional activity. Caspase-3 DNA binding enhanced angiogenesis by upregulating the expression of

proangiogenic genes and by activating pathways that promoted endothelial cell activation. Some proapoptotic genes were downregulated in caspase-3-proficient cells. Inhibiting caspase-3 increased the efficacy of chemotherapy and decreased spontaneous tumor development. These data highlight a novel nonapoptotic role of caspase-3 and suggest that cleaved caspase-3 could be a new therapeutic target in cancer.

Significance: These findings report a noncanonical function of caspase-3 by demonstrating its ability to transcriptionally regulate the VEGFR pathway.

Introduction

Apoptosis is a well-known physiologic process that enables the maintenance of homeostasis in multicellular organisms. Apoptosis can be induced by different stimuli such as cytotoxic drugs, irradiation, and hypoxic stress. One of the best-known markers of apoptosis is the proteolytic cleavage of pro-caspase-3 into its active form, caspase-3 (Casp-3). Once cleaved, Casp-3 translocates into the nucleus, where it cleaves specific substrates (1). Depending on the context, activation of Casp-3 is considered a deleterious event in different pathophysiologic processes, such as

neurodegenerative disorders or ischemia, or as a positive marker of effective therapeutic strategy such as in cancer. However, in recent years, new investigations have identified new nonapoptotic roles of caspases. Indeed, in cancer, activation of Casp-3 was described as a stimulator of tumor cell repopulation during radiotherapy treatment (2), or a driver of tumor cell proliferation in pancreatic cancer (3) and melanoma (4). Recently, Casp-3 was described as a mediator of neoangiogenesis in dying cells after X-ray therapy (5). Nevertheless, all nonapoptotic roles of Casp-3 rely on its proteolytic activity (6–9). In this article, we showed that Casp-3 activation induced transcriptional changes, leading to the upregulation of genes involved in angiogenesis and downregulation of genes involved in proapoptotic pathways. We have shown that Casp-3 was able to directly interact with the promoter of various proangiogenic genes, such as *VEGFA* gene, and induce transcription thanks to a specific DNA-binding domain. *In vivo*, the pharmacologic targeting of Casp-3 increased chemotherapy cytotoxicity in cancer cells.

Materials and Methods

Cell lines

All cell lines were cultured at 37°C under 5% CO₂. MCF7, MDA-MB-231, 4T1, and CT26 cells were obtained from ATCC. COLO-205 and HT29 cells sensitive and resistant to oxaliplatin were obtained from Pr. Olivier Adotevi and Pr Christophe Borg's lab (Inserm U1098, Besancon, France). MCF7, MCF7-Casp-3 (stably transfected), and MDA-MB-231 cells were cultured in DMEM (high glucose). 4T1, CT26, COLO-205, and HT-29 sensitive and resistant to oxaliplatin were cultured in RPMI1640. Mediums

¹Inserm U1231, Dijon, France. ²Department of Biology and Pathology of Tumors, Georges-Francois Leclerc Cancer Center—UNICANCER, Dijon, France. ³Platform of Transfer in Cancer Biology, Georges-Francois Leclerc Cancer Center—UNICANCER, Dijon, France. ⁴Preclinical Imaging Platform—Nuclear Medicine Department, Georges-Francois Leclerc Cancer Center—UNICANCER, Dijon, France. ⁵Pole of Pharmacology and Therapeutics, Institut de Recherche Expérimentale et Clinique, UCLouvain, Brussels, Belgium. ⁶Susan Lehman Cullman Laboratory for Cancer Research, Department of Chemical Biology, Ernest Mario School of Pharmacy, Rutgers, The State University of New Jersey, Piscataway, New Jersey. ⁷The Cancer Institute of New Jersey, New Brunswick, New Jersey.

Note: Supplementary data for this article are available at Cancer Research Online (<http://cancerres.aacrjournals.org/>).

Corresponding Author: Romain Boidot, Georges-Francois Leclerc Cancer Center-1, rue Professeur Marion, Dijon 21000, France. Phone: 333-8073-7767; Fax: 333-8073-7782; E-mail: rboidot@cgfl.fr

Cancer Res 2019;79:5958–70

doi: 10.1158/0008-5472.CAN-19-0840

©2019 American Association for Cancer Research.

were supplemented with 10% (vol/vol) FCS, 1% penicillin, streptomycin, and amphotericin B, 4 mmol/L HEPES. Colo-205 and HT-29 resistant to oxaliplatin were cultured with oxaliplatin at 3 $\mu\text{g}/\text{mL}$. Using concerning culture conditions of our MCF7 cells, experiments were performed simultaneously with MCF7 Casp-3^{-/-} and Casp-3^{+/+} within five cell subclonings. After five passages, new vials of both cells were thawed and new experiments were carried out. All cell lines were sequenced at the exome level and the transcriptomic level for authentication.

Next-generation sequencing

Total RNA was extracted with TRIzol reagent from MCF7 and Casp-3-transfected MCF7 cells treated or not with docetaxel. Libraries and analysis were performed as described previously (10). Chromatin immunoprecipitation (ChIP) sequencing was performed as described previously (11) for MCF7 or MCF7 Casp-3^{+/+} cells treated or not with docetaxel. Next-generation sequencing data are available on the GEO website with the SuperSeries reference: GSE87227.

Ethics approval and consent to participate

The study on patient samples was conducted in accordance with the Declaration of Helsinki and approved by the Ethics Committee of the Centre Georges-François Leclerc (Dijon, France), the Comité Consultatif de Protection des Personnes en Recherche Biomédicale de Bourgogne. Written informed consent was obtained from all patients before enrollment.

All the mice were maintained in specific pathogen-free conditions and all experiments followed the guidelines of the Federation of European Animal Science Associations. All animal experiments were approved by the Ethics Committee of Université de Bourgogne (Dijon, France).

In vivo experiments

MDA-MB-231 cells were cultured for 24 hours with control inhibitor as control or with the Casp-3 inhibitor, Z-DEVD-FMK. Then, 5×10^6 MDA-MB-231 cells in serum-free culture medium were inoculated subcutaneously into the right side of 8-week-old nude (nu/nu) BALB/c mice. As soon as tumors reached 400 mm², the mice were sacrificed and tumors were collected, included with optimal cutting temperature (OCT), and conserved at -80°C . Frozen sections were marked with CD31 antibody and DAPI.

BALB/c mice were subcutaneously injected with CT-26 or 4T1 cells and treated with 5-fluorouracil (50 mg/kg) + irinotecan (40 mg/kg) or docetaxel (10 mg/kg), respectively, 8 days after the tumor graft. Z-FA-FMK control inhibitor, Z-DEVD-FMK Casp-3 inhibitor, or anti-mouse VEGFA was injected intraperitoneally. siRNA transfections were performed twice a week as described previously (12) with anti-mouse pro-Casp-3 (GGATAGTGTTC-TAAGGAA), anti-mouse pro-caspase-6 (CCTGGTACATTCAG-GATTT), and anti-mouse pro-caspase-7 (CCTGTTAGAGAAACC-CAA) siRNA.

Twelve-week-old TG3 transgenic mice (13) had been intraperitoneally treated with Z-DEVD-FMK or Z-FA-FMK as a negative control for 4 months. Mice were sacrificed and tail tumor nodes were counted.

Statistical analysis

GraphPad Prism software was used for the statistical analysis. Statistical significance is shown as *, $P < 0.05$; **, $P < 0.01$; ***, $P < 0.001$; and ****, $P < 0.0001$.

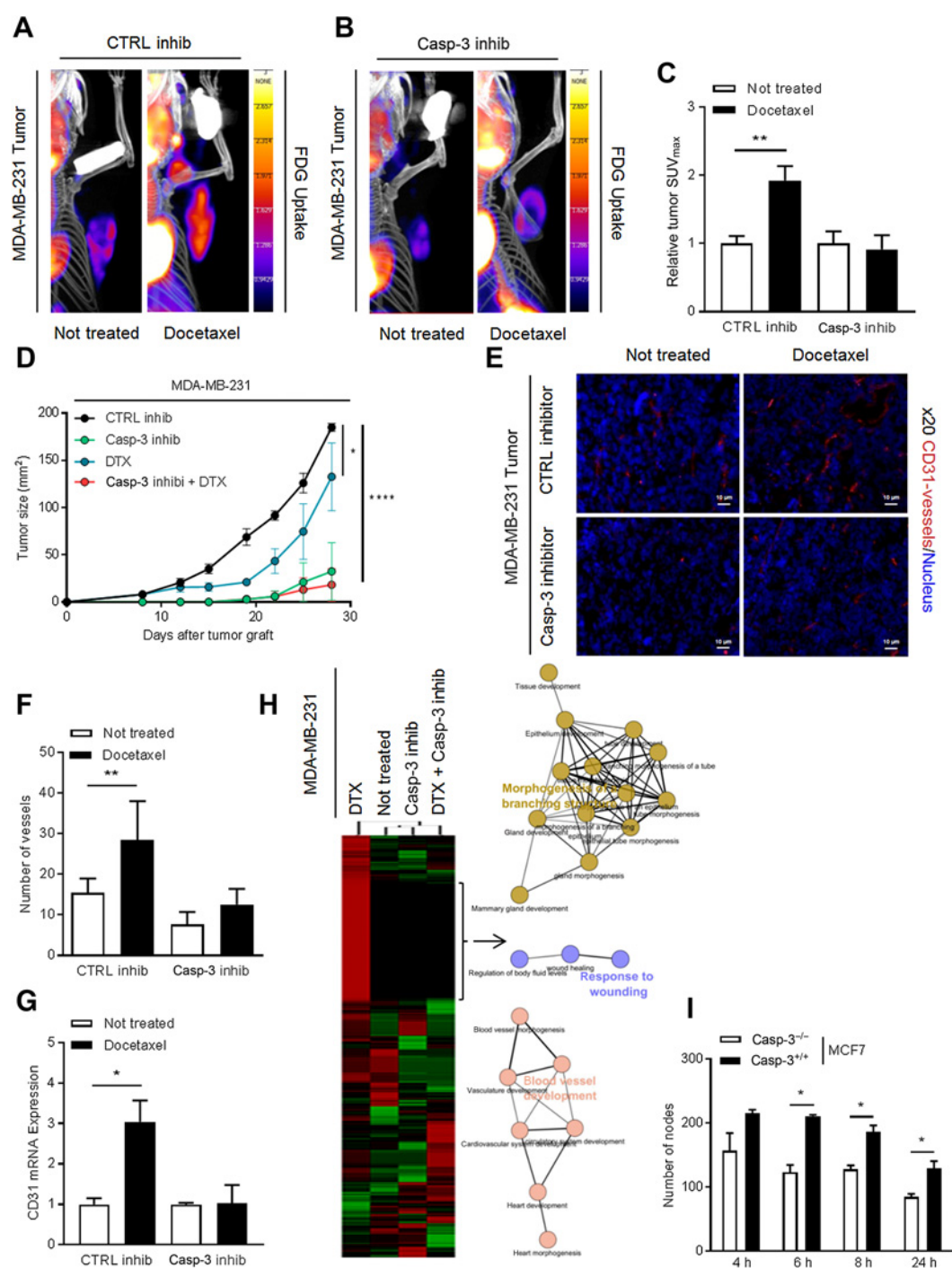
Results

Casp-3-dependent apoptosis is associated with tumor angiogenesis

It is known that an increase of standardized uptake value maximum (SUV_{max} corresponding to the ratio between tracer binding in the tumor on total injected radioactive activity normalized by the patient body weight) after one course of neoadjuvant docetaxel is a marker of nonresponse to treatment (14, 15). To understand the mechanism involved in the increase of SUV_{max} after docetaxel treatment, and consequently resistance to treatment, tumors generated with the aggressive MDA-MB-231 cells were treated or not with docetaxel. Two weeks later, FDG uptake was measured by PET scanner. First, we observed that docetaxel treatment induced FDG uptake compared with nontreated cells (Fig. 1A). As an increase of FDG uptake is correlated with tumor progression, we hypothesized that an inhibition of apoptosis by the pharmacologic Casp-3 inhibitor Z-DEVD-FMK would increase FDG uptake by tumors. Tumors treated by Casp-3 inhibitor alone presented a reduced size and, surprisingly, the inhibition of apoptosis completely abolished FDG uptake induced by docetaxel treatment (Fig. 1B and C). In agreement with literature, the decrease of FDG uptake, induced by Casp-3 inhibition, after one cycle of docetaxel was correlated with a decrease of tumor growth (Fig. 1D). As FDG uptake was described as being correlated with tumor angiogenesis (16), we wondered whether the result observed with FDG uptake was linked to tumor blood vessels. For that, we stained mouse blood vessels in the MDA-MB-231 tumors used for PET scanner experiments. We observed that docetaxel increased blood vessel density and that Casp-3 inhibitor treatment led to an inhibition of this phenomenon (Fig. 1E and F). In addition, quantification of tumor mouse vessels by CD31 mRNA expression analysis showed that docetaxel induced the expression of this blood vessel marker and that Casp-3 pharmacologic inhibition reduced its expression (Fig. 1G). To confirm that angiogenesis was impacted by docetaxel and Casp-3 pharmacologic inhibition, we performed RNA sequencing of human MDA-MB-231 injected into nude mice and treated or not with docetaxel \pm the Casp-3 inhibitor Z-DEVD-FMK. The sequences obtained were first aligned with the mouse genome. This enabled us to identify mechanisms induced by tumor cells in the host. Unsupervised clustering revealed that untreated tumors' profile was closer to that of tumors treated with the Casp-3 inhibitor Z-DEVD-FMK, or docetaxel and Z-DEVD-FMK than to that of tumors treated with docetaxel alone (Fig. 1H). ClueGO software analysis of a cluster of genes specifically induced in tumors treated with docetaxel alone revealed enrichment in genes involved in mechanisms known to promote angiogenesis (blood vessel development, morphogenesis of branching structures, and response to wounding; Fig. 1H).

We secondly aligned sequences with the human genome. By comparing treated and nontreated tumors, we observed that the treatment of MDA-MB-231 tumors with docetaxel-induced pathways involved in angiogenesis according to ClueGO analysis (Supplementary Fig. S1A). By performing additional analysis using Enrichr software (17, 18), we observed that numerous pathways inducing angiogenesis were significantly enriched in docetaxel-treated cells such as alpha adrenergic (19), oxytocin (20–22), thyrotropin (23), muscarinic receptor (24), p38 MAPK (25), 5-hydroxytryptamine (26), and platelet-derived growth factor (27) pathways (Supplementary Fig. S1B).

Bernard et al.

**Figure 1.**

Activation of Casp-3 stimulates angiogenesis. **A**, Images of FDG uptake experiment in mice previously injected with MDA-MB-231 cells cultured with Z-FA-FMK control inhibitor and treated or not with docetaxel (10 nmol/L). **B**, Images of FDG uptake experiment in mice previously injected with MDA-MB-231 cells cultured with Z-DEVD-FMK Casp-3 inhibitor and treated or not with docetaxel (10 nmol/L). **C**, Quantification of SUV_{max} calculated from analysis of FDG uptake. **D**, Tumor growth in nude BALB/c mice after subcutaneous injection of MDA-MB-231 cells preincubated with Z-FA-FMK control inhibitor or with Z-DEVD-FMK Casp-3 inhibitor, followed by intraperitoneal injection of docetaxel (10 mg/kg; *n* = 8 per group). Immunofluorescence staining analysis of OCT-embedded tumors from mice previously injected with MDA-MB-231 cells cultured with Z-FA-FMK control inhibitor or with Z-DEVD-FMK Casp-3 inhibitor and treated or not with docetaxel (10 nmol/L). CD31 vessels, red; nuclei, blue. **F**, Vessels quantification of immunofluorescence staining in **E**. **G**, RT-PCR analysis of CD31 expression in tumors in **E**. Data are presented as mean ± SD. **H**, Cluster and ClueGO software analysis showing RNA-sequencing data of human MDA-MB-231 injected into nude mice and treated or not with docetaxel (10 nmol/L) ± the Z-DEVD-FMK Casp-3 inhibitor. **I**, Number of nodes of HUVECs cultured or not with supernatant from MCF7 Casp-3^{-/-} or Casp-3^{+/+} cells. *, *P* < 0.05; **, *P* < 0.01; ****, *P* < 0.001.

To address the role of Casp-3–dependent cell death in angiogenesis, the naturally Casp-3–deficient cells (MCF7) were stably transfected with an empty vector (Casp3^{-/-}) or with a plasmid encoding Casp-3 cDNA (Casp-3^{+/+}). Both cell lines were treated with docetaxel at 10 nmol/L. This dose of docetaxel induced Casp-3 (Supplementary Fig. S1C) and caspase-9 (Supplementary Fig. S1D) cleavage in Casp-3^{+/+} cells with no differences observed neither in caspase-7 (Supplementary Fig. S1E) nor in caspase-8 (Supplementary Fig. S1F) cleavage nor in apoptosis (Supplementary Fig. S1G) nor in cell growth (Supplementary Fig. S1H) between both cell lines. After 24 hours of treatment, the medium containing docetaxel was removed; cells were washed and incubated for additional 24 hours with fresh docetaxel-free medium. Afterward, endothelial tube formation experiments were performed with the 24-hour conditioned drug-free cell medium. We observed that only docetaxel-treated Casp-3–proficient cells were able to induce tube formation and stabilize formed tubes (Fig. 1I). Altogether, these data suggest that Casp-3–dependent apoptosis could induce neovessel formation and its stabilization.

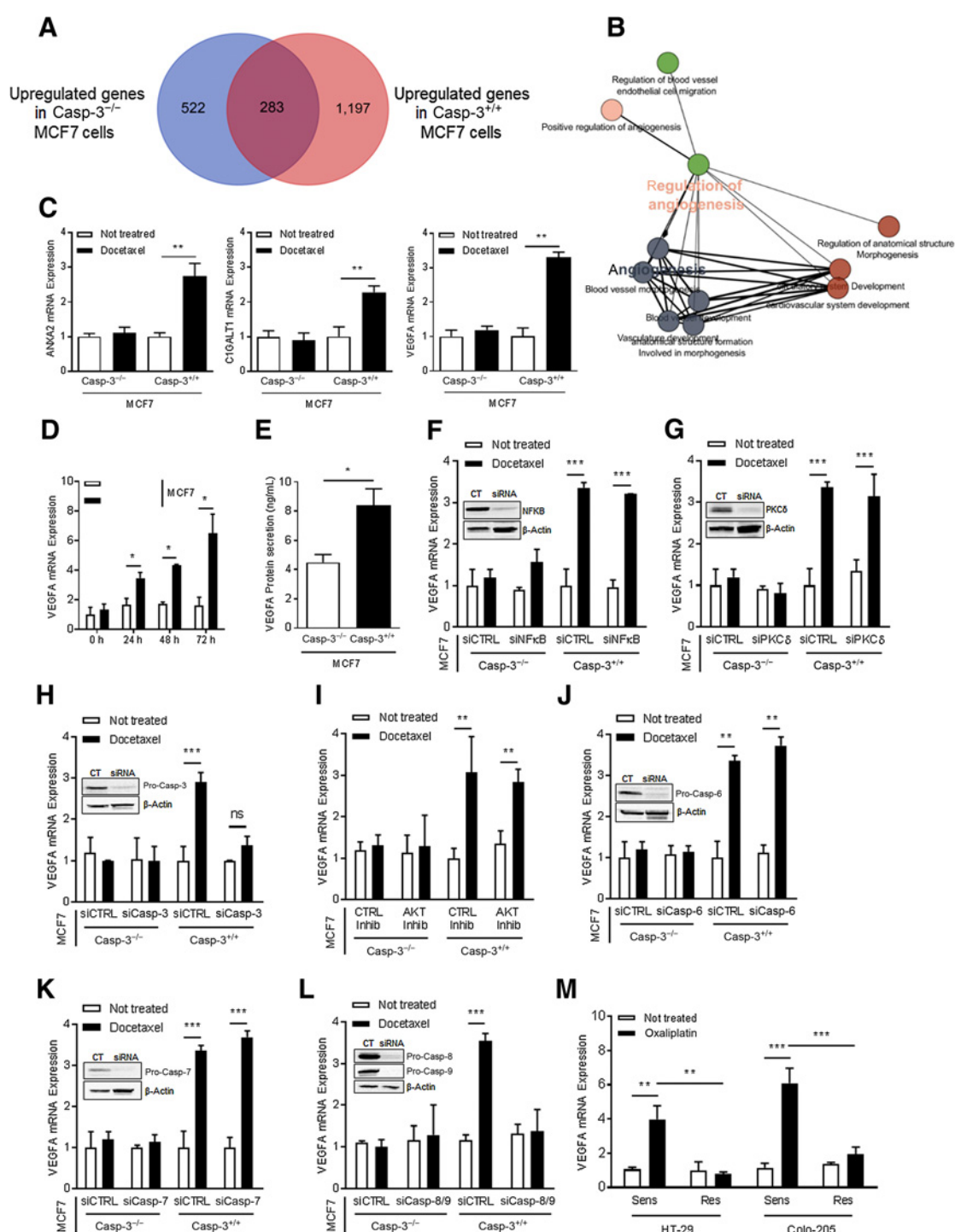
Activation of Casp-3 induces proangiogenic gene expression

We previously observed that apoptosis and particularly Casp-3–dependent apoptosis correlated with increased neovessel formation and vasculature stabilization. To decipher the mechanism involved in this phenomenon, we performed massive mRNA sequencing on Casp-3–deficient and Casp-3–proficient MCF7 cells treated with 10 nmol/L docetaxel as mentioned previously. This analysis allowed the identification of a set of 522 transcripts specifically upregulated in Casp-3–deficient cells, a set of 283 transcripts overexpressed in both cell lines, and a set of 1,197 transcripts specifically upregulated in Casp-3–proficient cells (Fig. 2A; Supplementary Table S1). Each subset had an enrichment of particular pathways as detected by Enrichr software. In the subset of 522 transcripts, four pathways were significantly enriched (Supplementary Fig. S2A), whereas in the subset of 283 transcripts, eight pathways were enriched (Supplementary Fig. S2B) as for the subset of 1,197 transcripts (Supplementary Fig. S2C). Interestingly, in the third subset, appeared a pathway named "Signaling events mediated by VEGFR1 and VEGFR2." Using ClueGO software, we confirmed that angiogenesis-related pathways were enriched in these 1,197 transcripts (Fig. 2B). As an example, the increased expression of the proangiogenic *ANXA2*, *C1GALT1*, and *VEGFA* genes was validated by qPCR exclusively in treated Casp-3–proficient cells (Fig. 2C). As *VEGFA* is a major proangiogenic gene involved in formation of neovessels and stabilization of vasculature, and as VEGFR1 and 2 signaling seemed activated only in Casp-3–proficient cells (Supplementary Fig. S2C), therefore, we decided to study its regulation by cleaved Casp-3 as an illustration of our observations. Although docetaxel cytotoxicity was identical in Casp-3–proficient and –deficient cells (Supplementary Fig. S1G and S1H), *VEGFA* mRNA expression increased continuously over time only in Casp-3–proficient cells (Fig. 2D), resulting in a higher *VEGFA* secretion in treated Casp-3–proficient cells (Fig. 2E) 72 hours after docetaxel treatment initiation (48 hours after docetaxel removal). Literature previously reported that *VEGFA* expression can be induced by NF- κ B (28) or Casp-3–activated PKC δ (29). Using specific siRNAs, we showed that neither NF- κ B (Fig. 2F) nor PKC δ (Fig. 2G) was involved in the *VEGFA* upregulation observed in our conditions. In contrast, extinction of Casp-3 by siRNA (Fig. 2H) or inhibition of Casp-3 activity by the pharmacologic inhibitor

Z-DEVD-FMK (Supplementary Fig. S2D) prevented *VEGFA* mRNA increase. In 2015, it was hypothesized that AKT phosphorylation was responsible for the induction of *VEGFA* expression in response to Casp-3 cleavage (5). In our experimental conditions, the pharmacologic inhibition of AKT activity had no effect on *VEGFA* expression (Fig. 2I). Once cleaved, Casp-3 cleaves and activates the 2 downstream caspases-6 and -7. Still with siRNA strategy, it appeared that neither caspase-6 (Fig. 2J) nor caspase-7 extinction (Fig. 2K) had an impact on the induction of *VEGFA* mRNA expression following docetaxel treatment of Casp-3–proficient cells. Casp-3 can share substrates with its downstream caspases, especially with caspase-7. To confirm that our observation was linked only to cleaved Casp-3, we pharmacologically inhibited Casp-3 in combination with siRNA strategy against Casp-3, caspase-6, or caspase-7. These experiments indicated that the Z-DEVD-FMK Casp-3 inhibitor lost its activity only in presence of the siRNA targeting Casp-3 (Supplementary Fig. S2E). To be active, Casp-3 needs to be cleaved by using upstream caspases, such as caspases-8 and -9. siRNA strategy targeting both upstream caspases, we surprisingly observed that both caspase-8 (Supplementary Fig. S2F) and caspase-9 (Supplementary Fig. S2G) extinction induced a slight decrease of *VEGFA* mRNA expression compared with treated control. Nevertheless, when both upstream caspases were downregulated, we observed a similar impact to that obtained with casp-3 inhibition (Fig. 2L). Indeed, upon docetaxel treatment, Casp-3 activation is triggered by both caspase-8 and caspase-9 (30). Consequently, silencing of both caspases-8 and -9 was required to prevent Casp-3 activation. Finally, we also tested whether *VEGFA* mRNA expression could be influenced by chemotherapy-induced Casp-3 activation, without external targeting of Casp-3. For that, we have used the two colon cancer cell lines HT-29 and Colo-205. For each cell line, we disposed of a sensitive versus a resistant oxaliplatin clone. Treatment by oxaliplatin induced Casp-3 activation and cell death only in sensitive clones and not in resistant ones. Thus, *VEGFA* induction in both cell lines was exclusively observed in the sensitive clone (Fig. 2M). Taken together, these results demonstrated that only cleaved Casp-3 was involved in the induction of *VEGFA* and by extension in proangiogenic gene expression in response to chemotherapy.

Cleaved Casp-3 binds DNA and induces transcription

We previously observed that activation of Casp-3 induced the expression of proangiogenic genes. As this induction seemed to be exclusively due to cleaved Casp-3 and as cleaved Casp-3 translocated into the nucleus under docetaxel treatment (Fig. 3A and B), we wondered whether cleaved Casp-3 could be able to interact with DNA. To elucidate this point, we performed ChIP sequencing (ChIP-seq) experiments by immunoprecipitating cleaved Casp-3 after docetaxel treatment in Casp-3–deficient MCF7 and Casp-3–proficient MCF7 cells. We first observed interactions between cleaved Casp-3 and DNA. These interactions were at 2% with gene promoters, 40% in intergenic regions, 30% in introns, and 1% in exons (Fig. 3C). From aligned data, we obtained three putative consensus DNA sequences of interaction between DNA and cleaved Casp-3 (Fig. 3D). Next, bioinformatics analyses revealed that cleaved Casp-3 interacted with 1,406 genes whose 117 genes had an expression induced only in the presence of Casp-3 (Fig. 3E; Supplementary Table S2). Among these 117 genes, the most enriched pathway was the "Signaling events mediated by VEGFR1 and VEGFR2" (Supplementary Fig. S3A),

**Figure 2.**

Activation of Casp-3 induces VEGFA expression. **A**, Venn diagram of an RNA sequencing analysis in Casp-3^{-/-} and Casp-3^{+/+} MCF7 cells 48 hours after docetaxel (10 nmol/L) treatment. **B**, Pathway activation analysis performed with the ClueGEO software from the 1,197 genes upregulated only in treated Casp-3-proficient MCF7 cells. **C**, RT-PCR analysis of ANXA2, CIGALT1, and VEGFA expression in Casp-3^{-/-} and Casp-3^{+/+} MCF7 cells treated or not with docetaxel (10 nmol/L). **D**, RT-PCR analysis of VEGFA expression at 0 hour, 24 hours, 48 hours, and 72 hours after the start of docetaxel treatment (10 nmol/L) in Casp-3^{-/-} and Casp-3^{+/+} MCF7 cells. **E**, ELISA of VEGFA secretion after docetaxel treatment (10 nmol/L) in Casp-3^{-/-} and Casp-3^{+/+} MCF7 cells. RT-PCR analysis of VEGFA mRNA expression from Casp-3^{-/-} and Casp-3^{+/+} MCF7 cells treated or not with docetaxel (10 nmol/L) and transfected with control siRNA or siRNAs targeting NF-κB (**F**), PKCδ (**G**), pro-Casp-3 (**H**), pro-caspase-6 (**J**), pro-caspase-7 (**K**), pro-caspase-8, and pro-caspase-9 (**L**), or treated with the AKT inhibitor ipatasertib (**I**) and corresponding immunoblot analysis testing the corresponding siRNA efficacy. **M**, RT-PCR analysis of VEGFA expression in HT-29 and Colo-205 cells sensitive or resistant to oxaliplatin and treated or not with oxaliplatin. Data are presented as mean ± SD. *, $P < 0.05$; **, $P < 0.01$; ***, $P < 0.001$; ns, nonsignificant.

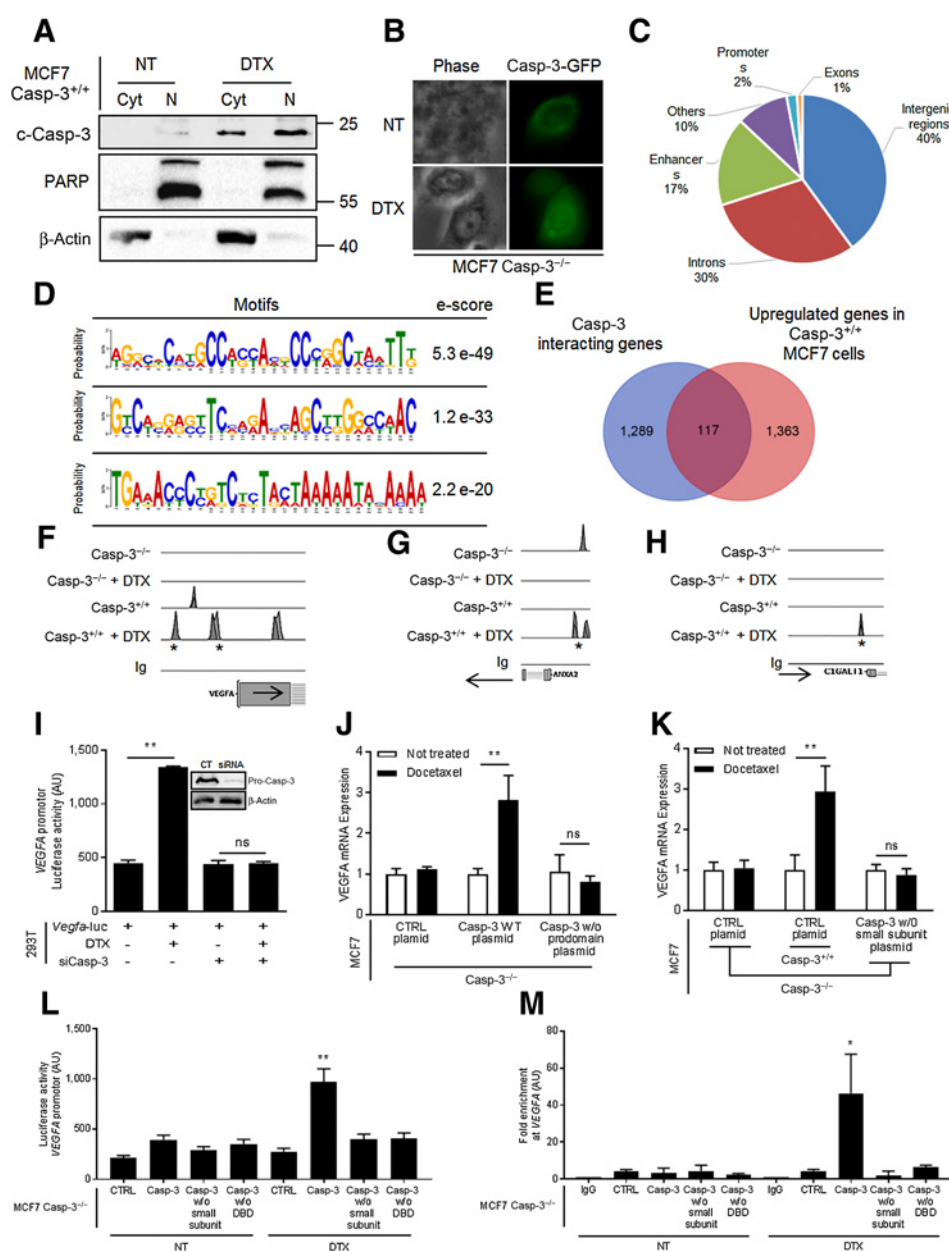
suggesting that cleaved Casp-3 was able to bind and activate genes involved in this pathway. Notably, ChIP-seq revealed an interaction between cleaved Casp-3 and the promoter of VEGFA (Fig. 3F), confirmed by ChIP PCR experiments (Supplementary Fig. S3B). We also observed that cleaved Casp-3 interacted with promoters of ANXA2 (Fig. 3G) and C1GALT1 (Fig. 3H), both induced in treated Casp-3-proficient cells (Fig. 2C). On the contrary, no interaction was observed with VEGFB and VEGFC promoters (Supplementary Fig. S3C) that were not induced by Casp-3 activation. As cleaved Casp-3 seemed to interact with DNA, we wondered whether this interaction was functional. Consequently, we performed luciferase assays. The transfection of the VEGFA promoter upstream from the luciferase gene was associated with luciferase signal detection only in presence of Casp-3 (Fig. 3I), whereas absence of pro-caspases-6 and -7 did not impact luciferase signal detection (Supplementary Fig. S3D). Pro-caspase-3 is structured in three main domains: a prodomain, a large subunit, and a small subunit (Supplementary Fig. S3E). To decipher the involvement of each pro-caspase-3 domain in the interaction between cleaved Casp-3 and DNA, we generated a Casp-3 protein without prodomain. This truncation induces a specific nuclear location of noncleaved Casp-3 (31). This prodomain-truncated Casp-3 did not induce any VEGFA mRNA expression after treatment into Casp-3-deficient cells, whereas the full-length Casp-3 did (Fig. 3J). This observation suggests that activation of Casp-3 by cleavage is necessary for its transcriptional activity. Similarly, we generated a Casp-3 protein lacking the small subunit. The expression of this second truncated form of Casp-3 in Casp-3-deficient cells was not associated with an increase of VEGFA mRNA (Fig. 3K). This result suggested that the interaction between cleaved Casp-3 and DNA needed the small subunit of Casp-3. Furthermore, we analyzed the catalytically inactive C163A isoform of Casp-3 that can adopt a conformation equivalent to wild-type Casp-3 but with no protease activity (32). Overexpression of this proteolytic-inactive mutant of Casp-3 induced VEGFA promoter activity as the wild-type Casp-3 (Supplementary Fig. S3F), suggesting that the catalytic activity of Casp-3 is not necessary for its transcriptional activity, contrarily to its conformation. Next, we wondered whether we could detect an amino acid sequence enabling an interaction with DNA. By using BindN tool (33), we observed the presence of a 15-amino acid sequence "AYSTAPGYYSWRNSK" with putative DNA interaction properties located in the small subunit of Casp-3 (Supplementary Fig. S3E). To test the DNA-binding ability of this 15 amino acid sequence, we generated a Casp-3 protein lacking the 15 amino acids and performed luciferase assays with the VEGFA promoter. The overexpression of the mutated Casp-3 was not able to induce luciferase activity in Casp-3-deficient cells (Fig. 3L) and completely abolished the luciferase activity induced by docetaxel (Supplementary Fig. S3G), even in the absence of caspases-3, -6, or -7 (Supplementary Fig. S3H). This observation suggested that this 15 amino acid sequence might be involved in DNA binding and consequently gene transcription induction by Casp-3 as the putative DNA-binding domain truncated Casp-3 was not able to interact with VEGFA promoter as demonstrated by ChIP experiment (Fig. 3H). Finally, as this putative DNA-binding domain is located in the small subunit of Casp-3 and as this small subunit was necessary for transcription induction, we wondered whether the small subunit alone was sufficient for transcription induction. We therefore generated a plasmid encoding only the small subunit of Casp-3 and performed a luciferase assay with the VEGFA

promoter. As obtained with the DNA-binding domain truncated Casp-3, overexpression of the small subunit alone did not induce luciferase activity in Casp-3-deficient cells (Fig. 3L), and no interaction between the small subunit of Casp-3 and the VEGFA promoter was observed (Fig. 3M). In Casp-3-proficient cells, the overexpression induced the same activation of the VEGFA promoter as the control (Supplementary Fig. S3I). Nevertheless, when we associated this overexpression with the extinction of caspases-3, -6, or -7, the activation of VEGFA promoter was completely abolished in absence of Casp-3 (Supplementary Fig. S3J), suggesting that the induction observed in Supplementary Fig. S3G was due to endogenous Casp-3. These results suggested that both subunits of cleaved Casp-3, and consequently a specific 3D structure of Casp-3, were required for the transcriptional activity of cleaved Casp-3.

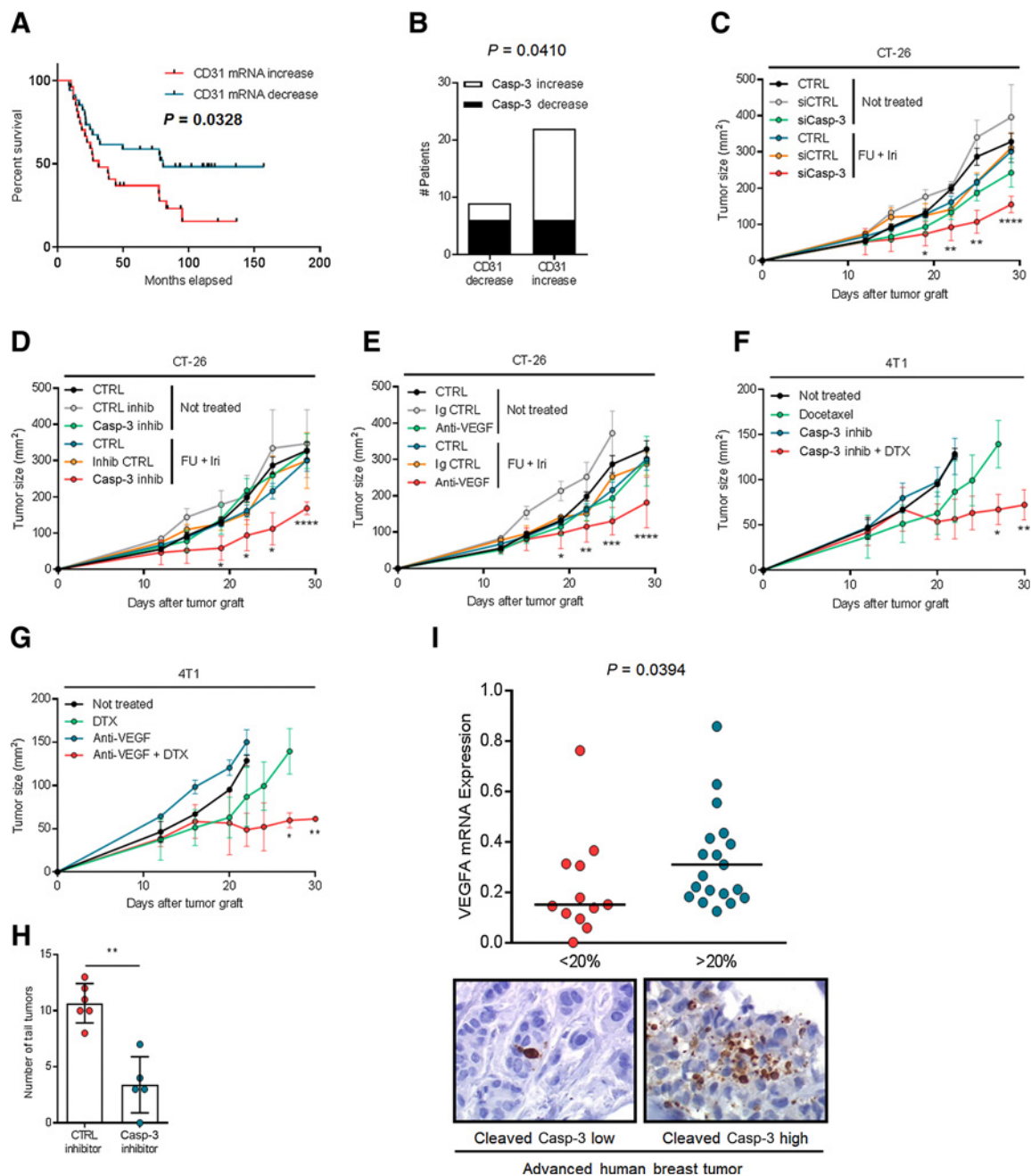
Casp-3 inhibition increases response to cytotoxic treatment

As described previously, we surprisingly observed that Casp-3 inhibition completely abolished the FDG uptake in tumors treated with docetaxel through angiogenesis inhibition. Moreover it also dramatically decreased tumor growth. These observations suggested that Casp-3 activation promoted aggressiveness of cancer cells by promoting neovessel formation and stabilization. To validate this observation in humans, we first studied the extent of the tumor vascular network, through the analysis of CD31 mRNA expression, before and after neoadjuvant chemotherapy in 61 locally advanced breast tumors and correlated data with relapse-free survival (RFS). We observed a significantly worse RFS in patients with increased CD31 mRNA expression after cytotoxic treatment than in patients with a decreased CD31 mRNA expression (Fig. 4A). On the same patients, we studied Casp-3 activation by IHC at the same time point. It appeared that the number of tumors with increased nuclear staining (Casp-3 cleavage) was about twice more than in tumors with decreased nuclear staining, indicating that neoadjuvant treatment induced Casp-3 activation. Moreover, 73% of tumors presenting increased CD31 expression also showed an increase of Casp-3 cleavage, and 67% of tumors with decreased CD31 expression showed a decrease of Casp-3 activation (Fig. 4B). This difference between both groups was statistically significant ($P = 0.041$). These findings indicated that neoadjuvant chemotherapy induced Casp-3 activation and that angiogenesis was increased in the majority of human breast tumors harboring Casp-3 activation. As the observations done in mouse were validated in humans, we wondered whether cleaved Casp-3 could be a therapeutic target. For that, we have used the mouse colon CT26 and mammary 4T1 cancer cell lines for *in vivo* experiments. Both mouse cell lines harbor the same behavior as human cell lines in response to Casp-3 activation by chemotherapy. Both increased VEGFA expression in response to cytotoxic treatment in the presence of cleaved Casp-3 (Supplementary Fig. S4A). *In vivo*, treatment of CT26 tumors with 5-fluorouracil + irinotecan did not affect tumor growth, whereas intratumor injection of anti-mouse Casp-3 siRNA alone slightly decreased tumor growth. Interestingly, the combination of siRNA with cytotoxic treatment dramatically increased the antitumor effects of 5-fluorouracil + irinotecan (Fig. 4C). In parallel, we also tested the impact of anti-mouse caspase-6 and anti-mouse caspase-7 siRNAs on tumor growth in absence and presence of cytotoxic treatment. Contrary to Casp-3 targeting, the targeting of caspase-6 and caspase-7 did not affect tumor growth (Supplementary Fig. S4B). The same observation was obtained with

Bernard et al.

**Figure 3.**

Cleaved Casp-3 binds DNA on a specific binding site, thanks to a DNA-binding domain. **A**, Immunoblot analysis of Casp-3^{-/-} and Casp-3^{+/+} MCF7 cells at 0 and 72 hours after docetaxel (10 nmol/L) treatment start, showing the subcellular distribution of cleaved Casp-3, with β-actin and PARP used as cytoplasmic and nuclear markers, respectively, to assess the purity of the fractionation. **B**, Fluorescence microscopy in Casp-3^{-/-} MCF7 cells transiently transfected with pro-Casp-3-GFP plasmid treated or not with docetaxel (10 nmol/L). **C**, Distribution of Casp-3 ChIP-seq peaks among various genome regions. **D**, Determination of Casp-3-binding motifs by analysis of Casp-3 ChIP-seq peaks from MCF7 Casp-3^{+/+} cells. Left, letter size indicates frequency of nucleotide. Right, significance of motif occurrence. **E**, Venn diagram showing the interaction between genes upregulated in Casp-3-proficient MCF7 cells and Casp-3-interacting genes. Casp-3-binding peaks identified by ChIP-seq on VEGFA (**F**), ANXA2 (**G**), and C1GALT1 (**H**) promoters in Casp-3^{-/-} and Casp-3^{+/+} MCF7 cells treated or not with docetaxel (10 nmol/L). Asterisks, interaction peaks between Casp-3 and the promoter; arrows, gene orientation. Blue and green colors correspond to read 1 and read 2 during sequencing run. **I**, Firefly luciferase activity in 293T cells after transfection of luciferase reporter constructs for the VEGFA promoter with various combinations of Casp-3-specific siRNA and docetaxel treatment (10 nmol/L), and immunoblot analysis testing transfection efficiency. **J**, RT-PCR analysis of VEGFA expression in Casp-3^{-/-} MCF7 cells treated or not with docetaxel (10 nmol/L) after transfection of plasmids encoding Casp-3 or prodomain-truncated Casp-3. **K**, RT-PCR analysis of VEGFA expression in Casp-3^{-/-} or Casp-3^{+/+} MCF7 cells treated or not with docetaxel (10 nmol/L) after transfection of plasmids encoding Casp-3 or Casp-3 without the small subunit. **L**, Firefly luciferase activity in Casp-3^{-/-} MCF7 cells transfected with plasmid encoding either pro-Casp-3, or the small subunit truncated Casp-3, or a DNA-binding domain truncated Casp-3, and then treated or not during 24 hours with docetaxel (10 nmol/L). **M**, ChIP-PCR analysis performed in Casp-3^{-/-} MCF7 cells transfected with plasmid encoding either pro-Casp-3, or the small subunit truncated Casp-3, or a DNA-binding domain truncated Casp-3, and then treated or not during 24 hours with docetaxel (10 nmol/L). Data are presented as mean ± SD. *, $P < 0.05$; **, $P < 0.01$.

**Figure 4.**

Caspase-3 inhibition increases response to cytotoxic treatment. **A**, Analysis of CD31 mRNA expression before and after neoadjuvant chemotherapy in 61 locally advanced breast tumors and correlated data with RFS. **B**, Graph representing the number of tumors presenting Casp-3 staining increase or decrease depending on CD31 expression variation (increase or decrease) after chemotherapeutic treatment. **C**, Tumor growth in BALB/c mice after subcutaneous injection of CT-26 cells, followed by intraperitoneal injections of 5-fluorouracil (FU; 50 mg/kg) and irinotecan (Iri; 40 mg/kg) with or without injections of Casp-3-specific siRNA into the tumor twice a week ($n = 8$ per group). **D**, Tumor growth in BALB/c mice after subcutaneous injection of CT-26 cells, followed by intraperitoneal injection of FU (50 mg/kg) and irinotecan (40 mg/kg) with weekly intraperitoneal injection of Z-FA-FMK control inhibitor or of Z-DEVD-FMK Casp-3 inhibitor ($n = 8$ per group). **E**, Tumor growth in BALB/c mice after subcutaneous injection of CT-26 cells, followed by intraperitoneal injection of FU (50 mg/kg) and irinotecan (40 mg/kg) with or without intraperitoneal injection of anti-mouse VEGFA-blocking antibody (one day after chemotherapy injection; $n = 8$ per group). **F**, Tumor growth in BALB/c mice after subcutaneous injection of 4T1 cells, followed by intraperitoneal injection of docetaxel (DTX; 10 mg/kg) with weekly intraperitoneal injection of Z-FA-FMK control inhibitor or with weekly intraperitoneal injection of Z-DEVD-FMK Casp-3 inhibitor ($n = 8$ per group). **G**, Tumor growth in BALB/c mice after subcutaneous injection of 4T1 cells, followed by intraperitoneal injection of docetaxel (10 mg/kg) with or without intraperitoneal injection of anti-mouse VEGFA blocking antibody (one day after chemotherapy injection; $n = 8$ per group). **H**, Number of tail tumors on TG3 mice treated or not with weekly intraperitoneal injection of Z-FA-FMK control inhibitor or Z-DEVD-FMK Casp-3 inhibitor for 4 months. **I**, Correlation between IHC analyses of Casp-3 activation in 31 locally advanced breast tumors and RT-PCR analysis of VEGFA expression. Data are presented as mean \pm SD. *, $P < 0.05$; **, $P < 0.01$; ***, $P < 0.001$; ****, $P < 0.0001$.

systemic inhibition of Casp-3 with the pharmacologic inhibitor Z-DEVD-FMK, administered intraperitoneally (Fig. 4D). Moreover, treatment of tumors with an anti-mouse VEGFA therapeutic antibody in association with chemotherapy showed the same benefit (Fig. 4E) as that observed with inhibition of Casp-3 by siRNA or the Z-DEVD-FMK inhibitor (Fig. 4C and D). Similar observations were obtained with the mammary 4T1 cancer cell model, where both inhibition of Casp-3 (Fig. 4F) and VEGFA targeting (Fig. 4G) further increased docetaxel growth inhibition.

In Fig. 1C, we observed that the pharmacologic inhibition of Casp-3 with Z-DEVD-FMK inhibitor strongly decreased tumorigenicity of highly tumorigenic MDA-MB-231 cancer cells. On the basis of the data previously described, we could hypothesize that cleaved Casp-3 promoted tumor development by inducing tumor angiogenesis through the induction of transcription of proangiogenic genes as VEGFA. To test this hypothesis, we wondered whether the pharmacologic inhibition of Casp-3, in a spontaneous melanoma mouse model, could decrease the development of tumors. The Casp-3 inhibitor Z-DEVD-FMK, or the control inhibitor Z-FA-FMK, was intraperitoneally injected once a week in 12-week-old TG3 mice. Four months later, mice were sacrificed and tail tumor nodes were counted. It appeared that mice treated with control Z-FA-FMK harbored a mean of 10 (7–12) nodes, whereas mice treated with the Casp-3 inhibitor Z-DEVD-FMK had a mean of only 3.4 (0–7) nodes (Fig. 4H), confirming that activation of Casp-3 could be tumorigenic. Finally, we wondered whether Casp-3 activation, detected by IHC in 31 locally advanced breast tumors, could be correlated with an increased VEGFA mRNA expression. We observed that tumors with a low Casp-3 activation (less than 20% of stained nuclei) harbored a significantly lower expression of VEGFA mRNA than did tumors with high Casp-3 activation (more than 20% of stained nuclei; Fig. 4I).

Cleaved Casp-3 possibly downregulates antiapoptotic genes

Using data obtained from massive RNA sequencing comparing Casp-3-deficient and Casp-3-proficient cells treated or not with docetaxel, we observed that treated Casp-3-proficient cells specifically downregulated 486 genes. The analysis of these downregulated genes indicated a significant enrichment of eight pathways (Fig. 5A). Surprisingly, among these eight pathways specifically downregulated in treated Casp-3-proficient cells, seven were involved in apoptosis induction: FAS, TRAIL, IFN γ , ceramide, TNF receptor, RAC1, and Tap63 pathways. This observation suggested that the activation of Casp-3 decreases the expression of genes inducing apoptosis, especially extrinsic apoptosis. As we previously showed that cleaved Casp-3 was able to bind DNA and promote gene transcription, we wondered whether it was also able to inhibit transcription of proapoptotic genes by direct interaction with DNA. For that, we compared the list of the 486 downregulated genes with the list of the 1,407 Casp-3-interacted genes. Among the 36 genes common between both lists (Fig. 5B), no pathways were significantly enriched (Fig. 5C), suggesting that the mechanism underlying downregulation was not due to a direct interaction of Casp-3 with DNA. We then focused on genes present in enriched pathways of Fig. 5A. Sixteen genes were represented in these downregulated pathways: *ARRB1*, *BIRC2*, *DHRS3*, *GPX2*, *IQGAP1*, *IRF1*, *MAP3K1*, *MAP3K11*, *NQO1*, *PIK3CB*, *PKN1*, *PRKCD*, *RACGAP1*, *RIPK1*, *SMPD1*, and *ZYX* (Fig. 5D). Among these 16 genes, except *RACGAP1* for which Casp-3 interacted with an enhancer region of this gene, none was a target of Casp-3 DNA-binding activity (Fig. 5E), suggesting that

these downregulations were probably due to an indirect mechanism. However, the analysis of these 15 genes without interaction with Casp-3 showed that their expression was mainly under the control of two transcription factors: NFE2L2 and FOXA2, suggesting that a putative indirect mechanism explaining downregulation of antiapoptotic genes in Casp-3-proficient cells might be an inhibition of NFE2L2 and FOXA2 (Fig. 5F).

Discussion

One of the hallmarks of cancer is resistance to apoptosis (34), suggesting that apoptosis induction in cancer cells is an important anticancer mechanism. Since a few years, some works tend to demonstrate that caspases' activation (6–8, 35), and especially Casp-3 (2, 4, 5, 9, 36–38), could have impact independently of apoptosis that could even have inverse effects on cell death. In this work, we showed that apoptosis-triggering Casp-3 activation is responsible for transcriptional changes such as upregulation and downregulation of some genes compared with apoptosis in absence of Casp-3. Among upregulated genes, we observed that some genes involved in angiogenesis, another hallmark of cancer, were significantly represented. This overexpression of genes, such as VEGFA, the main driver of angiogenesis, was correlated with an increased angiogenesis *in vivo*. This observation is in agreement with two previous studies, which showed that Casp-3 activation was linked to angiogenesis induction in a hepatocyte model (39) and in a cancer model after treatment with ionizing radiations (5). Consequently, we decided to focus on VEGFA expression as an illustration of Casp-3 transcriptional activity. We showed that the induction of VEGFA was exclusively due to cleaved Casp-3 and not NF- κ B (28) in our experimental conditions. Our observation could be explained by the proteolytic cleavage and therefore inhibition of NF- κ B by cleaved Casp-3 (40), contrary to the angiogenesis stimulated by Casp-8 in glioblastoma that is due to NF- κ B activation (41).

Our results also contradict the hypotheses that the induction of angiogenesis by Casp-3 requires the activating proteolytic cleavage of PKC δ by Casp-3 (29), or AKT activation (5, 29). Our results could be in accordance with different studies. Indeed, PKC δ was shown to induce stabilization of VEGFA translation without impacting its transcription (42). Moreover, AKT was described as a target of cleaved Casp-3, inducing an abolishment of its activity (43, 44). As once cleaved, Casp-3 translocates into the nucleus, we wondered whether the induction of proangiogenic genes could be due to an unexpected transcriptional function of cleaved Casp-3. After its proteolytic activation, Casp-3 migrates to the nucleus and directly interacts with DNA, especially in regions containing proangiogenic genes, to induce transcription. This interaction needs the 15 amino acid motif "AYSTAPGYYSWRNSK" and the formation of the tertiary structure between small and large subunits of Casp-3. Nevertheless, the proteolytic activity of Casp-3 is not necessary for its transcriptional activity, as the overexpression of the inactive C163A Casp-3 isoform was able to induce VEGFA expression to the same extent as wild-type Casp-3. We demonstrate that cleaved Casp-3 translocates into the nucleus for a function other than its canonical proteolytic activity. Moreover, we confirmed a link between Casp-3 activation and angiogenesis in breast tumors. Almost 75% of breast tumors presenting an increase in CD31 mRNA after chemotherapy also showed an increase in Casp-3 activation. Besides, increased angiogenesis could be related to a worse RFS in breast

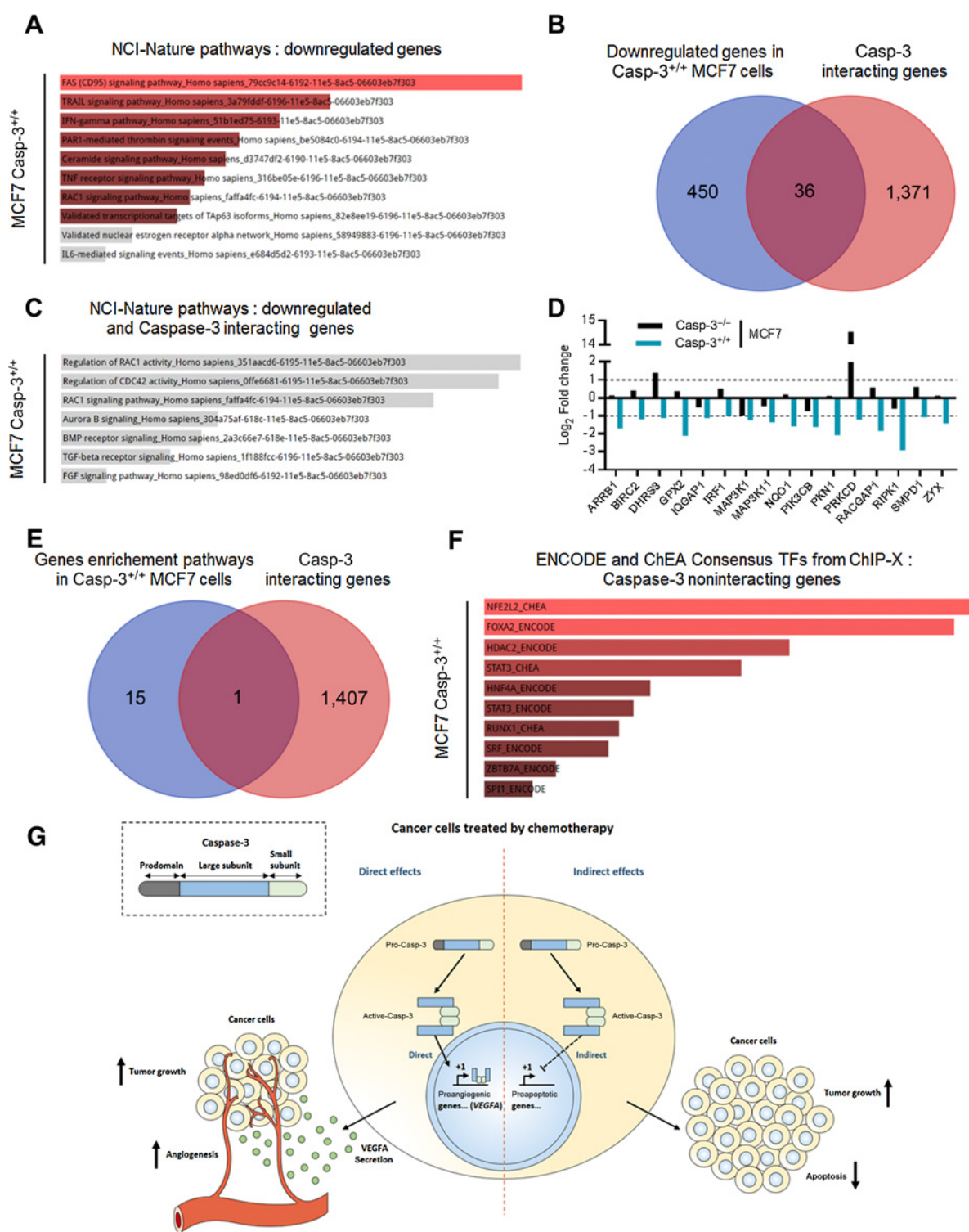


Figure 5. Cleaved Casp-3 could downregulate antiapoptotic genes. **A**, RNA-sequencing analysis of MCF7 Casp-3^{+/+} downregulated genes with Enrichr NCI-Nature pathway database. **B**, Venn diagram of genes downregulated in Casp-3^{+/+} MCF7 cells and Casp-3-interacted genes. **C**, RNA-sequencing analysis of the 36 genes in common in **B** with Enrichr NCI-Nature pathway database. **D**, Fold change of enriched genes in **A** showing RNA-sequencing data of Casp-3^{+/+} and Casp-3^{-/-} MCF7 cells. **E**, Venn diagram of enriched genes in Casp-3^{+/+} MCF7 cells and Casp-3-interacted genes. **F**, RNA-sequencing analysis Casp-3 noninteracting genes in MCF7 Casp-3^{+/+} cells with Enrichr ENCODE and ChEA Consensus TFs from ChIP-X. **G**, Suggested model for Casp-3 direct effects on proangiogenic genes and indirect effects on proapoptotic genes.

tumors. In addition to its role in the induction of angiogenesis, VEGFA is also described as an inducer of resistance in cancer cells (45). Recently, VEGFA (46) and Casp-3 (47) were associated with the development of fibrosis in pancreatic cancer, a marker of resistance to chemotherapeutic treatment (48). VEGFA has also been associated with an increased infiltration of immunosuppressive cells, myeloid-derived suppressor cell, in ovarian cancer, resulting in local immunity inhibition and a poor prognosis (49). In parallel with the direct upregulation of genes, Casp-3 was also able to induce downregulation of other genes, some involved in proapoptotic pathways. This downregulation was not due to a direct interaction with promoters but possibly through the inhibition of NFE2L2 and FOXA2. At the transcriptional level, FOXA2 was not detected in our RNA-seq analysis, whereas NFE2LE was. The inhibition of NFE2L2 could be due to its cleavage by cleaved Casp-3 as described in HeLa cells during TNF α -mediated apoptosis (50). This double effect of Casp-3 activation (upregulation of proangiogenic genes and downregulation of proapoptotic genes) could explain the observation showing that Casp-3 inhibition improved chemotherapy efficacy. Consequently Casp-3 can be a new therapeutic target. Moreover, this double effect could explain that Casp-3 targeting could prevent tumor growth in mice but also tumor development in genetically predisposed mice, suggesting that Casp-3 inhibition could be a prophylactic treatment for patients with a familial risk of cancer. The therapeutic use of Casp-3 inhibitors could be rapidly tested in clinics as a feasibility study was performed for the use of Casp-3 inhibitors in *Pemphigus vulgaris* (51), and a randomized clinical trial of emricasan, a pan-caspase inhibitor, was performed in subjects with nonalcoholic fatty liver disease (52).

Our data indicate that Casp-3 could be a therapeutic target to enhance the efficacy of chemotherapy. In contrast, in other medical domains such as neurodegenerative diseases or ischemic disorders of heart or brain, our data could encourage the development of Casp-3-protective treatments. Indeed, in cases of myocardial infarction, Casp-3 is rapidly cleaved (53), resulting in a putative induction of proangiogenic genes and decrease of proapoptotic genes, which could protect cardiac muscle (54, 55). In a previous study, we showed that the inhibition of caspase-6 blocked apoptosis without blocking Casp-3 activation (12). In these conditions, we could speculate that the inhibition of caspase-6 could block the deleterious impact of apoptosis on heart cells without affecting the benefit of Casp-3 activation on the production of other proangiogenic factors. A similar rationale could be applied to ischemic stroke, in which cleaved Casp-3 is essential for neuroprotection (56) and an increase in VEGFA is neuroprotective (57). Finally, VEGF stimulates neural stem cells'

proliferation after cerebral ischemia and could enable the treatment of neurodegenerative disorders (58–60).

Our study highlights unexpected functions of Casp-3 in cells. Indeed, we showed that cleaved Casp-3 is able to interact with DNA and more specifically with promoters of proangiogenic genes. This interaction induces transcription of these genes and leads to neoangiogenesis (Fig. 5G). In parallel, activation of Casp-3 induced, by an indirect mechanism, downregulation of genes involved in proapoptotic pathways. These observations could explain why the activation of Casp-3 is required for tumorigenesis and is a factor of resistance to cytotoxic drugs (Fig. 5G). Finally, we identified cleaved Casp-3 as a new therapeutic target in cancer as its inhibition sensitizes cells to chemotherapy drugs and decreases the development of tumors in genetically predisposed mice.

Disclosure of Potential Conflicts of Interest

No potential conflicts of interest were disclosed.

Authors' Contributions

Conception and design: L. Apetoh, F. Végran, R. Boidot

Development of methodology: S. Chevrier, V. Déragère, F. Végran, R. Boidot

Acquisition of data (provided animals, acquired and managed patients, provided facilities, etc.): A. Bernard, S. Chevrier, F. Beltjens, M. Dosset, E. Viltard, A. Lagrange, A. Oudot, B. Collin, L. Apetoh, O. Feron, S. Chen, L. Arnould, F. Végran, R. Boidot

Analysis and interpretation of data (e.g., statistical analysis, biostatistics, computational analysis): A. Bernard, F. Beltjens, A. Lagrange, A. Oudot, B. Collin, L. Arnould, F. Végran, R. Boidot

Writing, review, and/or revision of the manuscript: L. Apetoh, O. Feron, S. Chen, L. Arnould, F. Végran, R. Boidot

Administrative, technical, or material support (i.e., reporting or organizing data, constructing databases): F. Ghiringhelli, R. Boidot

Study supervision: R. Boidot

Acknowledgments

We thank Pr. Christophe Borg and Pr. Olivier Adotevi for supplying oxaliplatin-sensitive and -resistant clones of Colo-205 and HT-29 cell lines. We thank Dr. Alexia Cotte for her critical read of the manuscript and Isabel Gregoire for manuscript editing. We also thank "Ligue contre le Cancer de Côte d'Or" and "Ligue contre le Cancer de Saône-et-Loire" for the financial support of this work. We thank "Ligue contre le Cancer" for financially supporting A. Bernard. Imaging experiments were supported by a French Government Grant managed by the French National Research Agency (ANR) under the program "Investissements d'Avenir" (reference ANR-10-EQPX-05-01/IMAPPI Equipex).

The costs of publication of this article were defrayed in part by the payment of page charges. This article must therefore be hereby marked *advertisement* in accordance with 18 U.S.C. Section 1734 solely to indicate this fact.

Received March 12, 2019; revised July 17, 2019; accepted October 8, 2019; published first October 14, 2019.

References

- Kamada S, Kikkawa U, Tsujimoto Y, Hunter T. Nuclear translocation of caspase-3 is dependent on its proteolytic activation and recognition of a substrate-like protein(s). *J Biol Chem* 2005;280:857–60.
- Huang Q, Li F, Liu X, Li W, Shi W, Liu FF, et al. Caspase 3-mediated stimulation of tumor cell repopulation during cancer radiotherapy. *Nat Med* 2011;17:860–6.
- Cheng J, Tian L, Ma J, Gong Y, Zhang Z, Chen Z, et al. Dying tumor cells stimulate proliferation of living tumor cells via caspase-dependent protein kinase C δ activation in pancreatic ductal adenocarcinoma. *Mol Oncol* 2015;9:105–14.
- Donato AL, Huang Q, Liu X, Li F, Zimmerman MA, Li CY. Caspase 3 promotes surviving melanoma tumor cell growth after cytotoxic therapy. *J Invest Dermatol* 2014;134:1686–92.
- Feng X, Tian L, Zhang Z, Yu Y, Cheng J, Gong Y, et al. Caspase 3 in dying tumor cells mediates post-irradiation angiogenesis. *Oncotarget* 2015;6:32353–67.
- Boege Y, Malehmir M, Healy ME, Bettermann K, Lorentzen A, Vucur M, et al. A dual role of caspase-8 in triggering and sensing proliferation-associated DNA damage, a key determinant of liver cancer development. *Cancer Cell* 2017;32:342–59.
- Mukherjee A, Williams DW. More alive than dead: non-apoptotic roles for caspases in neuronal development, plasticity and disease. *Cell Death Differ* 2017;24:1411–21.
- Gorelick-Ashkenazi A, Weiss R, Sapozhnikov L, Florentin A, Tarayrah-Ibraheim L, Dweik D, et al. Caspases maintain tissue integrity by an apoptosis-independent inhibition of cell migration and invasion. *Nat Commun* 2018;9:2806.

9. Yosefzon Y, Soteriou D, Feldman A, Kostic L, Koren E, Brown S, et al. Caspase-3 regulates YAP-dependent cell proliferation and organ size. *Mol Cell* 2018;70:573–87.
10. Vegran F, Berger H, Boidot R, Mignot G, Bruchard M, Dosset M, et al. The transcription factor IRF1 dictates the IL-21-dependent anticancer functions of TH9 cells. *Nat Immunol* 2014;15:758–66.
11. Bruchard M, Rebe C, Derangere V, Togbe D, Ryffel B, Boidot R, et al. The receptor NLRP3 is a transcriptional regulator of TH2 differentiation. *Nat Immunol* 2015;16:859–70.
12. Vegran F, Mary R, Gibeaud A, Mirjole C, Collin B, Oudot A, et al. Survivin-3B potentiates immune escape in cancer but also inhibits the toxicity of cancer chemotherapy. *Cancer Res* 2013;73:5391–401.
13. Pollock PM, Cohen-Solal K, Sood R, Namkoong J, Martino JJ, Koganti A, et al. Melanoma mouse model implicates metabotropic glutamate signaling in melanocytic neoplasia. *Nat Genet* 2003;34:108–12.
14. Hirakata T, Yanagita Y, Fujisawa T, Fujii T, Kinoshita T, Horikoshi H, et al. Early predictive value of non-response to docetaxel in neoadjuvant chemotherapy in breast cancer using 18F-FDG-PET. *Anticancer Res* 2014;34:221–6.
15. Coudert B, Pierga JY, Mouret-Reynier MA, Kerrou K, Ferrero JM, Petit T, et al. Use of [(18)F]-FDG PET to predict response to neoadjuvant trastuzumab and docetaxel in patients with HER2-positive breast cancer, and addition of bevacizumab to neoadjuvant trastuzumab and docetaxel in [(18)F]-FDG PET-predicted non-responders (AVATAXHER): an open-label, randomised phase 2 trial. *Lancet Oncol* 2014;15:1493–502.
16. Kaira K, Oriuchi N, Shimizu K, Ishikita T, Higuchi T, Imai H, et al. Correlation of angiogenesis with 18F-FMT and 18F-FDG uptake in non-small cell lung cancer. *Cancer Sci* 2009;100:753–8.
17. Chen EY, Tan CM, Kou Y, Duan Q, Wang Z, Meirelles GV, et al. Enrichr: interactive and collaborative HTML5 gene list enrichment analysis tool. *BMC Bioinformatics* 2013;14:128.
18. Kuleshov MV, Jones MR, Rouillard AD, Fernandez NF, Duan Q, Wang Z, et al. Enrichr: a comprehensive gene set enrichment analysis web server 2016 update. *Nucleic Acids Res* 2016;44(W1):W90–7.
19. Chen H, Liu D, Yang Z, Sun L, Deng Q, Yang S, et al. Adrenergic signaling promotes angiogenesis through endothelial cell-tumor cell crosstalk. *Endocr Relat Cancer* 2014;21:783–95.
20. Cattaneo MG, Chini B, Vicentini LM. Oxytocin stimulates migration and invasion in human endothelial cells. *Br J Pharmacol* 2008;153:728–36.
21. Cattaneo MG, Lucci G, Vicentini LM. Oxytocin stimulates in vitro angiogenesis via a Pyk-2/Src-dependent mechanism. *Exp Cell Res* 2009;315:3210–9.
22. Zhu J, Wang H, Zhang X, Xie Y. Regulation of angiogenic behaviors by oxytocin receptor through Gli1-induced transcription of HIF-1 α in human umbilical vein endothelial cells. *Biomed Pharmacother* 2017;90:928–34.
23. Hoffmann S, Hofbauer LC, Scharrenbach V, Wunderlich A, Hassan I, Lingelbach S, et al. Thyrotropin (TSH)-induced production of vascular endothelial growth factor in thyroid cancer cells in vitro: evaluation of TSH signal transduction and of angiogenesis-stimulating growth factors. *J Clin Endocrinol Metab* 2004;89:6139–45.
24. de la Torre E, Davel L, Jasnis MA, Gotoh T, de Lustig ES, Sales ME. Muscarinic receptors participation in angiogenic response induced by macrophages from mammary adenocarcinoma-bearing mice. *Breast Cancer Res* 2005;7:R345–52.
25. Rajashekhar G, Kamocka M, Marin A, Suckow MA, Wolter WR, Badve S, et al. Pro-inflammatory angiogenesis is mediated by p38 MAP kinase. *J Cell Physiol* 2011;226:800–8.
26. Machida T, Iizuka K, Hirafuji M. 5-hydroxytryptamine and its receptors in systemic vascular walls. *Biol Pharm Bull* 2013;36:1416–9.
27. Raica M, Cimpean AM. Platelet-derived growth factor (PDGF)/PDGF receptors (PDGFR) axis as target for antitumor and antiangiogenic therapy. *Pharmaceuticals* 2010;3:572–99.
28. Shibata A, Nagaya T, Imai T, Funahashi H, Nakao A, Seo H. Inhibition of NF- κ B activity decreases the VEGF mRNA expression in MDA-MB-231 breast cancer cells. *Breast Cancer Res Treat* 2002;73:237–43.
29. Cheng J, He S, Wang M, Zhou L, Zhang Z, Feng X, et al. The caspase-3/PKC δ /Akt/VEGF-A signaling pathway mediates tumor repopulation during radiotherapy. *Clin Cancer Res* 2019;25:3732–43.
30. Jelinek M, Balusikova K, Schmiedlova M, Nemcova-Furstova V, Sramek J, Stancikova J, et al. The role of individual caspases in cell death induction by taxanes in breast cancer cells. *Cancer Cell Int* 2015;15:8.
31. Luo M, Lu Z, Sun H, Yuan K, Zhang Q, Meng S, et al. Nuclear entry of active caspase-3 is facilitated by its p3-recognition-based specific cleavage activity. *Cell Res* 2010;20:211–22.
32. Tawa P, Hell K, Giroux A, Grimm E, Han Y, Nicholson DW, et al. Catalytic activity of caspase-3 is required for its degradation: stabilization of the active complex by synthetic inhibitors. *Cell Death Differ* 2004;11:439–47.
33. Wang L, Brown SJ. BindN: a web-based tool for efficient prediction of DNA and RNA binding sites in amino acid sequences. *Nucleic Acids Res* 2006;34 (Web Server issue):W243–8.
34. Hanahan D, Weinberg RA. Hallmarks of cancer: the next generation. *Cell* 2011;144:646–74.
35. Nakajima YI, Kuranaga E. Caspase-dependent non-apoptotic processes in development. *Cell Death Differ* 2017;24:1422–30.
36. Kim JS, Ha JY, Yang SJ, Son JH. A novel non-apoptotic role of procaspase-3 in the regulation of mitochondrial biogenesis activators. *J Cell Biochem* 2018;119:347–57.
37. Yosefzon Y, Fuchs Y. Exiting the dark side: a vital role for Caspase-3 in Yap signaling. *Mol Cell Oncol* 2018;5:e1494947.
38. Feng X, Yu Y, He S, Cheng J, Gong Y, Zhang Z, et al. Dying glioma cells establish a proangiogenic microenvironment through a caspase 3 dependent mechanism. *Cancer Lett* 2017;385:12–20.
39. Povero D, Eguchi A, Niesman IR, Andronikou N, de Mollerat du Jeu X, Mulya A, et al. Lipid-induced toxicity stimulates hepatocytes to release angiogenic microparticles that require Vanin-1 for uptake by endothelial cells. *Sci Signal* 2013;6:ra88.
40. Kang KH, Lee KH, Kim MY, Choi KH. Caspase-3-mediated cleavage of the NF- κ B subunit p65 at the NH2 terminus potentiates naphthoquinone analog-induced apoptosis. *J Biol Chem* 2001;276:24638–44.
41. Fianco G, Mongiardì MP, Levi A, De Luca T, Desideri M, Triscioglio D, et al. Caspase-8 contributes to angiogenesis and chemotherapy resistance in glioblastoma. *Elife* 2017;6. doi: 10.7554/eLife.22593.
42. Sataranatarajan K, Lee MJ, Mariappan MM, Feliars D. PKC δ regulates the stimulation of vascular endothelial factor mRNA translation by angiotensin II through hnRNP K. *Cell Signal* 2008;20:969–77.
43. Jahani-Asl A, Basak A, Tsang BK. Caspase-3-mediated cleavage of Akt: involvement of non-consensus sites and influence of phosphorylation. *FEBS Lett* 2007;581:2883–8.
44. Chu J, Lauretti E, Pratico D. Caspase-3-dependent cleavage of Akt modulates tau phosphorylation via GSK3 β kinase: implications for Alzheimer's disease. *Mol Psychiatry* 2017;22:1002–8.
45. Ge YL, Zhang X, Zhang JY, Hou L, Tian RH. The mechanisms on apoptosis by inhibiting VEGF expression in human breast cancer cells. *Int Immunopharmacol* 2009;9:389–95.
46. Yang L, Kwon J, Popov Y, Gajdos GB, Ordog T, Brekken RA, et al. Vascular endothelial growth factor promotes fibrosis resolution and repair in mice. *Gastroenterology* 2014;146:1339–50.
47. Laplante P, Sirois I, Raymond MA, Kokta V, Beliveau A, Prat A, et al. Caspase-3-mediated secretion of connective tissue growth factor by apoptotic endothelial cells promotes fibrosis. *Cell Death Differ* 2010;17:291–303.
48. Erkan M, Reiser-Erkan C, Michalski CW, Kleeff J. Tumor microenvironment and progression of pancreatic cancer. *Exp Oncol* 2010;32:128–31.
49. Horikawa N, Abiko K, Matsumura N, Hamanishi J, Baba T, Yamaguchi K, et al. Expression of vascular endothelial growth factor in ovarian cancer inhibits tumor immunity through the accumulation of myeloid-derived suppressor cells. *Clin Cancer Res* 2017;23:587–99.
50. Ohtsubo T, Kamada S, Mikami T, Murakami H, Tsujimoto Y. Identification of NRF2, a member of the NF-E2 family of transcription factors, as a substrate for caspase-3(-like) proteases. *Cell Death Differ* 1999;6:865–72.
51. Hariton WVJ, Galichet A, Vanden Berghe T, Overmiller AM, Mahoney MG, Declercq W, et al. Feasibility study for clinical application of caspase-3 inhibitors in Pemphigus vulgaris. *Exp Dermatol* 2017;26:1274–7.
52. Shiffman M, Freilich B, Vuppalanchi R, Watt K, Chan JL, Spada A, et al. Randomised clinical trial: emricasan versus placebo significantly decreases ALT and caspase 3/7 activation in subjects with non-alcoholic fatty liver disease. *Aliment Pharmacol Ther* 2019;49:64–73.

Bernard et al.

53. Schwarz K, Simonis G, Yu X, Wiedemann S, Strasser RH. Apoptosis at a distance: remote activation of caspase-3 occurs early after myocardial infarction. *Mol Cell Biochem* 2006;281:45–54.
54. Ai F, Chen M, Li W, Yang Y, Xu G, Gui F, et al. Danshen improves damaged cardiac angiogenesis and cardiac function induced by myocardial infarction by modulating HIF1alpha/VEGFA signaling pathway. *Int J Clin Exp Med* 2015;8:18311–8.
55. Ai F, Chen M, Yu B, Yang Y, Xu G, Gui F, et al. Puerarin accelerate cardiac angiogenesis and improves cardiac function of myocardial infarction by upregulating VEGFA, Ang-1 and Ang-2 in rats. *Int J Clin Exp Med* 2015;8:20821–8.
56. McLaughlin B, Hartnett KA, Erhardt JA, Legos JJ, White RF, Barone FC, et al. Caspase 3 activation is essential for neuroprotection in preconditioning. *Proc Natl Acad Sci U S A* 2003;100:715–20.
57. Yang ZJ, Bao WL, Qiu MH, Zhang LM, Lu SD, Huang YL, et al. Role of vascular endothelial growth factor in neuronal DNA damage and repair in rat brain following a transient cerebral ischemia. *J Neurosci Res* 2002;70:140–9.
58. Lambrechts D, Carmeliet P. VEGF at the neurovascular interface: therapeutic implications for motor neuron disease. *Biochim Biophys Acta* 2006;1762:1109–21.
59. Cariboni A, Davidson K, Dozio E, Memi F, Schwarz Q, Stossi F, et al. VEGF signalling controls GnRH neuron survival via NRP1 independently of KDR and blood vessels. *Development* 2011;138:3723–33.
60. Vijayalakshmi K, Ostwal P, Sumitha R, Shruthi S, Varghese AM, Mishra P, et al. Role of VEGF and VEGFR2 receptor in reversal of ALS-CSF induced degeneration of NSC-34 motor neuron cell line. *Mol Neurobiol* 2015;51:995–1007.

Cancer Research

The Journal of Cancer Research (1916–1930) | The American Journal of Cancer (1931–1940)

Cleaved Caspase-3 Transcriptionally Regulates Angiogenesis-Promoting Chemotherapy Resistance

Antoine Bernard, Sandy Chevrier, Françoise Beltjens, et al.

Cancer Res 2019;79:5958-5970. Published OnlineFirst October 14, 2019.

Updated version Access the most recent version of this article at:
doi:[10.1158/0008-5472.CAN-19-0840](https://doi.org/10.1158/0008-5472.CAN-19-0840)

Supplementary Material Access the most recent supplemental material at:
<http://cancerres.aacrjournals.org/content/suppl/2019/10/12/0008-5472.CAN-19-0840.DC1>

Cited articles This article cites 59 articles, 10 of which you can access for free at:
<http://cancerres.aacrjournals.org/content/79/23/5958.full#ref-list-1>

E-mail alerts [Sign up to receive free email-alerts](#) related to this article or journal.

Reprints and Subscriptions To order reprints of this article or to subscribe to the journal, contact the AACR Publications Department at pubs@aacr.org.

Permissions To request permission to re-use all or part of this article, use this link
<http://cancerres.aacrjournals.org/content/79/23/5958>.
Click on "Request Permissions" which will take you to the Copyright Clearance Center's (CCC) Rightslink site.